

On the gravitational potential of the Earth's lithosphere

David D. Coblenz and Randall M. Richardson

Southern Arizona Seismic Observatory, Department of Geosciences, University of Arizona, Tucson

Michael Sandiford

Department of Geology and Geophysics, University of Adelaide, Adelaide, Australia

Abstract. The mean potential energy of the lithosphere \bar{U}_l^g is useful for defining the tectonic reference state (TRS) of the Earth and can be used to constrain the ambient state of stress in the plates. In the absence of external forces applied at the base or along plate boundaries a lithospheric column with the potential energy of the TRS would remain undeformed. Thus the difference between the potential energy of a lithospheric column and the TRS determines whether the column is in an extensional, neutral, or compressional state of stress. We evaluate \bar{U}_l^g and intraplate variations about this mean, using a simple, first-order lithospheric density model. This model assumed that the continental geotherm is linear, and density variations below a depth of 125 km have negligible influence on \bar{U}_l^g , and is consistent with observed geoid anomalies across continental margins. \bar{U}_l^g is estimated to be $2.379 \times 10^{14} \text{ N m}^{-1}$, which is equivalent to the potential energy of both near sea level continental lithosphere (-160 to +220 m for an assumed crustal density, ρ_c , in the range $2800 - 2700 \text{ kg m}^{-3}$) and cooling oceanic lithosphere at a depth of 4.3 km. With the exception of Eurasia, which has anomalously high mean potential energy ($\bar{U}_l^p = 2.383 \times 10^{14} \text{ N m}^{-1}$), the mean potential energies of the continental plates are nearly identical to the global mean \bar{U}_l^g . The mean potential of the oceanic plates was found to be a strong function of the mean age of the oceanic lithosphere. Both the global and plate mean potential energies are relatively insensitive to a wide range in ρ_c . The potential of the mid-ocean ridges (U_l^{MOR}), $2.391 \times 10^{14} \text{ N m}^{-1}$, is greater than the global mean, which is consistent with the divergent nature of the ridges. Elevated continental lithosphere with a height of about 70 m has an equivalent potential energy to \bar{U}_l^g , suggesting that in the absence of external forces, continental regions will be in a slightly extensional state of stress. The importance of our potential energy formulation is substantiated by the strong correlation between the torque poles associated with the potential energy distributions and the observed plate velocity poles for the South American, Nazca, Indo-Australian, and Pacific plates.

Copyright 1994 by the American Geophysical Union.

Paper number 94TC01033.
0278-7407/94/94TC-01033\$10.00

Introduction

Lateral density variations in the lithosphere have long been associated with variations in lithospheric gravitational potential energy and are recognized as an important source of intraplate stress and associated deformation [e.g., Frank, 1972; Artyushkov, 1973; Lister, 1975; Molnar and Tapponier, 1978; Houseman, et al. 1981; England and McKenzie, 1982; Fleitout and Froidevaux, 1982, 1983; England, 1987; Zhou and Sandiford, 1992]. The excess potential energy associated with high topography [Molnar and Lyon-Caen, 1988] and mid-ocean ridges [Parsons and Richter, 1980; Dahlen, 1981] has been used to explain the extensional nature of these features.

We postulate that information about the mean potential energy of the lithosphere \bar{U}_l provides a way to understand the tectonic state of stress (compressional, neutral, or extensional) at both global and plate scales. In attempting to understand the stress associated with gravitational potential energy variations, it is useful to first define a tectonic reference state (TRS). In general, a lithospheric column in potential and isostatic balance with the TRS will remain undeformed in the absence of external forces. We assume that the reference lithosphere is isostatically compensated at or beneath its base. Isostasy does not specify a complete force balance, however, and it has often been assumed that the reference continental lithosphere is in potential energy balance with mid-ocean ridges [e.g., Turcotte et al., 1977; McKenzie, 1978; Le Pichon and Angelier, 1979; Cochran, 1982; Le Pichon, 1983; Turcotte, 1983; Crough, 1983; Houseman and England, 1986; Sonder et al., 1987; England and Houseman, 1988, 1989; Zhou and Sandiford, 1992]. The extensional nature of mid-ocean ridges, however, implies that they are in a state of excess potential energy, and it would be more appropriate to define the TRS in terms of \bar{U}_l .

The principal aim of the present study is to provide an approximate formulation for the potential energy distribution of the lithosphere at both global and plate scales in order to constrain the TRS. The main difficulty with addressing the potential energy of the Earth's lithosphere arises from uncertainties in our knowledge of the density structure, particularly in the continental crust,

and one of our main aims is to assess the sensitivity of our estimates of both global and plate mean potential energy to such uncertainties. Our calculations are based on a simple, first-order model of the lithosphere which reflects density variations associated with topographic features at a $1^\circ \times 1^\circ$ resolution. We have extended our initial estimates [Richardson and Coblenz, 1992] by the use of a more realistic density structure for the lithosphere based on the assumption of a linear geotherm, using reference densities for the crust and mantle that satisfy constraints imposed by observed geoid anomalies across continental margins. We discuss some insights into the origin of the stress fields of plates with active mountain belts by utilizing the concept of the TRS. Finally, we evaluate the correlation between the torque poles associated with the potential energy distributions and the observed plate velocity poles for the individual plates.

Tectonic Stresses due to Lateral Density Variations

On a global scale, horizontal stresses due to lateral density variations are known to be a major contributor to the intraplate stress field through ridge push, which is one of the principal driving mechanisms for plate tectonics. This force arises from the cooling and thickening of oceanic lithosphere with age and has been estimated to be of the order of $3 \times 10^{12} \text{ N m}^{-1}$ of ridge length [Frank, 1972; Lister, 1975; Parsons and Richter, 1980]. Note that since ridge push arises from lateral density variations within the oceanic lithosphere, it is an intraplate source of stress rather than a plate boundary force [Frank, 1972]. The results of a number of studies have confirmed the relationship between the ridge push force and intraplate stress orientations [e.g., Richardson et al., 1979; Richardson and Cox, 1984; Richardson and Reding, 1991; Wortel et al., 1991; Richardson, 1992]. The slab pull force also arises from density variations but, in this case, between subducted lithosphere and the surrounding sublithospheric mantle. The fact that the global intraplate stress data set [Zoback et al., 1992] of over 8000 stress indicators is dominated by compressional and strike-slip indicators implies, however, that the surface plates do not feel the large slab pull. This is consistent with a large, oppositely directed slab resistance acting locally on the slab [Forsyth and Uyeda, 1975]. Thus while slab pull is an important component of the driving mechanism, other processes such as lateral density variations within the plates play a central role in nature of the intraplate stress field.

An example of these other processes includes the buoyancy force due to crustal density variations associated with high topography and continental margins. The buoyancy forces associated with the generation of high topography in continents can be several times larger than the ridge push force [e.g., Fleitout

and Froidevaux, 1982, 1983; Molnar and Lyon-Caen, 1988; Fleitout, 1991; Zoback and Magee, 1991; Sandford and Powell, 1990, 1991; Zhou and Sandford, 1992] and are thought to be responsible for the normal stress regime in regions such as the Altiplano and the Tibetan plateaus. Similarly, stresses arising from lateral density variations at passive continental margins can perturb the regional stress field and locally alter the tectonic style of deformation [Coblenz and Richardson, 1992].

Gravitational Potential Energy of the Lithosphere

The gravitational potential energy per unit area of a column of material U above a given depth z is given by the integral of the vertical stress σ_{zz} from z to the surface h [e.g., Molnar and Lyon-Caen, 1988]

$$U = \int_z^h \sigma_{zz}(\tau) d\tau = g \int_z^h \int_\tau^h \rho(\tau') d\tau' d\tau \quad (1)$$

where $\rho(z)$ is the density at depth z ; h is the surface elevation; and g is the gravitational acceleration. The potential energy of the lithospheric column U_l is defined by (1) when z corresponds to the equipotential surface at which the lithosphere is compensated z_{iso} . For the purpose of this study it is useful to define the mean potential energy of the lithosphere at both the global scale $\overline{U^g}$ and the plate scale $\overline{U_l^p}$.

Because the lithosphere can be considered to be in isostatic equilibrium for wavelengths greater than a few hundred kilometers [Kaula, 1970, 1972; Turcotte and McAdoo, 1979; Sandwell and Smith, 1992], horizontal stresses can be directly related to the vertical density distribution [Hazby and Turcotte, 1978; Dahlen, 1981]

$$\overline{\sigma_{xx}} = \frac{g}{L} \int_h^L \Delta \rho(z) z dz \quad (2)$$

where z is the depth; L is the lithospheric thickness; and $\overline{\sigma_{xx}}$ is the horizontal stress averaged over the thickness of the lithosphere, relative to a reference state against which the $\Delta \rho$ is measured. Equation (2) shows that the mean horizontal stress is related to the local dipole moment of the density distribution M

$$\overline{\sigma_{xx}} = \frac{g}{L} M \quad (3)$$

Using the definition of gravitational potential energy in (1), the horizontal stress can be expressed in terms of the potential energies

$$\overline{\sigma_{xx}} = \frac{\Delta U_l}{L} \quad (4)$$

where ΔU_l is the difference between the potential energy of the local lithospheric column U_l and the poten-

tial energy of some column defining a reference tectonic state U_r

$$\Delta U_l = U_l - U_r$$

To a good approximation, geoid anomalies in isostatically compensated regions can also be related to the density moment [Haxby and Turcotte, 1978; Turcotte and Schubert, 1982]. Thus the geoid height anomaly provides valuable, independent information which can be used to constrain the density distribution within the lithosphere. The geoid anomaly can be expressed as [Turcotte and Schubert, 1982]

$$\Delta N = -\frac{2\pi G}{g} \int_h^L \Delta \rho(z) z dz \quad (5)$$

where G is the gravitational constant. ΔN can be rewritten in terms of the potential energy differences ΔU_l

$$\Delta N = -\frac{2\pi G}{g^2} \Delta U_l \quad (6)$$

As will be seen later, the relationship between the geoid height anomaly and lithospheric potential energy gradients provides an important constraint on the density structure of the continental lithosphere. These simple linear expressions are a good approximation when the density anomalies are in isostatic equilibrium, as is assumed in the present study.

Lithospheric Density Models

The calculation of U_l requires information about the density structure of the lithosphere about which there is considerable uncertainty, particularly in the continental crust. The purpose here is to devise a first-order view of the potential energy distribution, and thus a very simple density structure was assumed (in defense of the simplistic assumptions it will be shown that the main results are robust to the principal uncertainty, which is the reference density for the continental crust ρ_c). For the purpose of the present study the lithosphere has been categorized into four principal types (young oceanic, oceanic basin, submerged continent, and exposed continent) based on global topographic (ETOPO5 [National Geophysical Data Center, 1988]) and seafloor age information [Royer et al., 1992].

For each of these lithospheric types a thermally stabilized mantle lithosphere was assumed, and simple density distribution appropriate to a linear geotherm was used, with the density of the crust defined by

$$\rho_c(z) = \rho_c \{1 + \alpha_v [T_l - T(z)]\} \quad (7)$$

and in the mantle lithosphere

$$\rho_m(z) = \rho_m \{1 + \alpha_v [T_l - T(z)]\} \quad (8)$$

where ρ_c and ρ_m are the crustal density and mantle density, respectively, at T_l , the temperature at the base

of the lithosphere; and α_v is the thermal expansion coefficient. Because the average surface elevation of the lithosphere at length scales appropriate to local isostatic compensation reflects the local density structure of the lithosphere, the lithospheric density structure for each of the four lithospheric types has been formulated in terms of topography (or bathymetry), with a few simple assumptions about the nature of isostatic mechanism (see appendix A). The density distribution for the lithosphere is based on the following assumptions: (1) the lithosphere columns are in local isostatic equilibrium, and (2) the contribution to the potential energy variations from lateral density variations beneath a depth of 125 km below sea level is negligible. Therefore it is assumed that the equipotential surface appropriate to global isostatic compensation z_{iso} is 125 km below sea level. This is equivalent to assuming that the thickness of the lithosphere is about 125 km [Turcotte and McAdoo, 1979; Morgan and Smith, 1992]. Further constraints used for the lithospheric types are described below.

Young Oceanic Lithosphere

For the purposes of the present study, young oceanic lithosphere was assumed to predate the end of the Cretaceous normal megapolarity epoch at 84 Ma, which approximately corresponds to the age where the subsidence of oceanic lithosphere is not predicted by the half-space cooling model [e.g., Turcotte and Schubert, 1982; Morgan and Smith, 1992].

The potential energy for a lithospheric column of young oceanic material was calculated assuming that the thickness of the oceanic crust is constant. Consequently, variations in bathymetry are correlated with variations in the thickness of the lithosphere (where the base of the lithosphere is defined by the intercept of the lithospheric conductive geotherm and the mantle adiabatic temperature T_l). At the ridge the thickness of the lithosphere is assumed to be that of the oceanic crust. The bathymetry of normal oceanic ridges is assumed to be 2.5 km. The oceanic crust is assumed to have a thickness of 7 km [White et al., 1992] and a density of 2960 kg m^{-3} at the reference temperature T_l . The density of the asthenosphere constrained by Pratt isostacy was constrained to be 3238 kg m^{-3} . The effects on mantle density of melt extraction from the upper part of the mantle during the formation of the oceanic crust have been ignored in this formulation [e.g., Oxburgh and Parmentier, 1977].

Oceanic Basin

The ocean basins were assumed to have a constant lithospheric thickness with base at depth 125 km below sea level ($= z_{iso}$), consistent with the thermal plate model [Parsons and Sclater, 1977]. To account for potential energy variations associated with anomalously shallow regions of the ocean basins such as seamounts,

variations were allowed in thickness of the oceanic crust to preserve local isostatic balance with the mid-ocean ridges.

Continental Margins

In this formulation the lithospheric density structure for the submerged continental margins (oceanic regions close to the continents with bathymetry less than 2000 m) and exposed continents differs only in the incorporation of the contribution of the water column in the former. In both cases, variation in topography (or bathymetry) is assumed to reflect variations in crustal thickness assuming the base of the lithosphere, at T_l , is fixed at $z_{iso} = 125$ km depth. This formulation represents a significant approximation, since the elevated topography in some areas of the continents is likely compensated by anomalously hot mantle rather than thick crust, as for example, in the Basin and Range Province of the western United States. In appendix B it is shown that for regions of continents with elevated topography, of the order of 1 – 3 km above sea level, the assumed mechanism of isostatic support, whether it be variation in the thickness of the mantle lithosphere or of the crust, results in only minor variations in the potential energy of the lithospheric column, and therefore this approximation does not significantly affect the results. A significant uncertainty regarding the continental lithospheric density structure pertains to the crustal density ρ_c , which is known to be heterogeneous across a wide range of scales. As described in the following section, the density of the continental crust ρ_c relative to oceanic lithosphere is constrained by modeling the observed geoid anomalies across the ocean-continent margins.

Representative lithospheric columns for each of the lithospheric types are shown as Figure 1. Each $1^\circ \times 1^\circ$ region of the Earth's surface was categorized as one of the four lithospheric types (on the basis of age in the oceanic regions and on bathymetry in the case of continental margins) and U_l was calculated by evaluating (1) for the appropriate topography (or bathymetry). The parameters used to evaluate U_l are listed in Table 1 [Parsons and Sclater, 1977; Turcotte and McAdoo, 1979; Turcotte and Schubert, 1982]. The full expressions used for the calculation of the potential energy for each of the lithospheric types are given in appendix A.

Constraint on the Density of the Continental Crust

The strong dependence of U_l on the near-surface density distribution makes it critical to constrain the value of ρ_c . Figure 2 shows that this dependence of U_l on ρ_c is particularly strong for continental lithosphere with high elevation.

For lithospheric columns supporting 4 km of elevation this difference in potential energies amounts to 6.7

$\times 10^{12}$ N m $^{-1}$ for ρ_c equal to 2600 and 2900 kg m $^{-3}$, respectively, but diminishes to only 1×10^{12} N m $^{-1}$ for lithospheric columns supporting 1 km of elevation. Indeed, the recognition of the sensitive dependence of the potential energy on ρ_c for lithospheric columns supporting high elevation led *England and Molnar* [1991] to suggest that it was pointless to attempt direct calculation of potential energies from topography alone, as is proposed here. While this dependence of U_l on ρ_c does have important consequences for the range in intraplate potential energy which dictates the magnitude of the local lithospheric stress state, it will be shown that it has a relatively small effect on the global and plate mean potential energies $\overline{U_l^g}$, due to the relatively small amount of elevated topography greater than 1 km.

While admitting there may be considerable regional variation in crustal density values within the continents, one way to constrain typical mean crustal densities is to use independent information from geoid anomalies [e.g., *Turcotte and Schubert*, 1982]. As discussed above (e.g., (5)), the geoid anomaly can be directly related to the local dipole moment of the density-depth distribution and thus provides an independent constraint on ρ_c . The geoid anomaly across passive Atlantic-style continental margins has been estimated to be about 6 m [*Hazby and Turcotte*, 1978; *Turcotte and McAdoo*, 1979; *Turcotte and Schubert*, 1982; *Coblenz and Richardson*, 1992]. Predicted geoid anomaly across the continental margin calculated from (5) for ρ_c in the range of 2600 to 2900 kg m $^{-3}$ are listed in Table 2. There is close agreement between the observed and predicted geoid anomaly for a value of ρ_c in the range of 2700 to 2800 kg m $^{-3}$. Unless otherwise stated, a value of 2750 kg m $^{-3}$ for ρ_c is used in the following calculations.

Global-Scale and Plate-Scale Lithospheric Potential Energy Estimates

Global bathymetry and topography information was obtained from the ETOPO5 topographic data set. The average bathymetry or topography was calculated for surface elements of dimension $1^\circ \times 1^\circ$ (about 12,300 km 2 at the equator). Thus the effect of isolated seamounts and other anomalous topographic features on the mean elevation can be considered to be negligible. While the bathymetric information in the ETOPO5 data set has been shown to contain large errors [Smith, 1993], the use of the average bathymetry within $1^\circ \times 1^\circ$ windows minimizes the effect of these errors on this analysis.

Histograms of the topographic distributions for the entire Earth and the seven major plates (Africa, Eurasia, Indo-Australia, North America, South America, Pacific, and Nazca) are shown in Figure 3a, while the surface areas, average elevations, and percentages of the plates composed of young oceanic, old oceanic, continental margin, and exposed continental lithosphere are listed in Table 3.

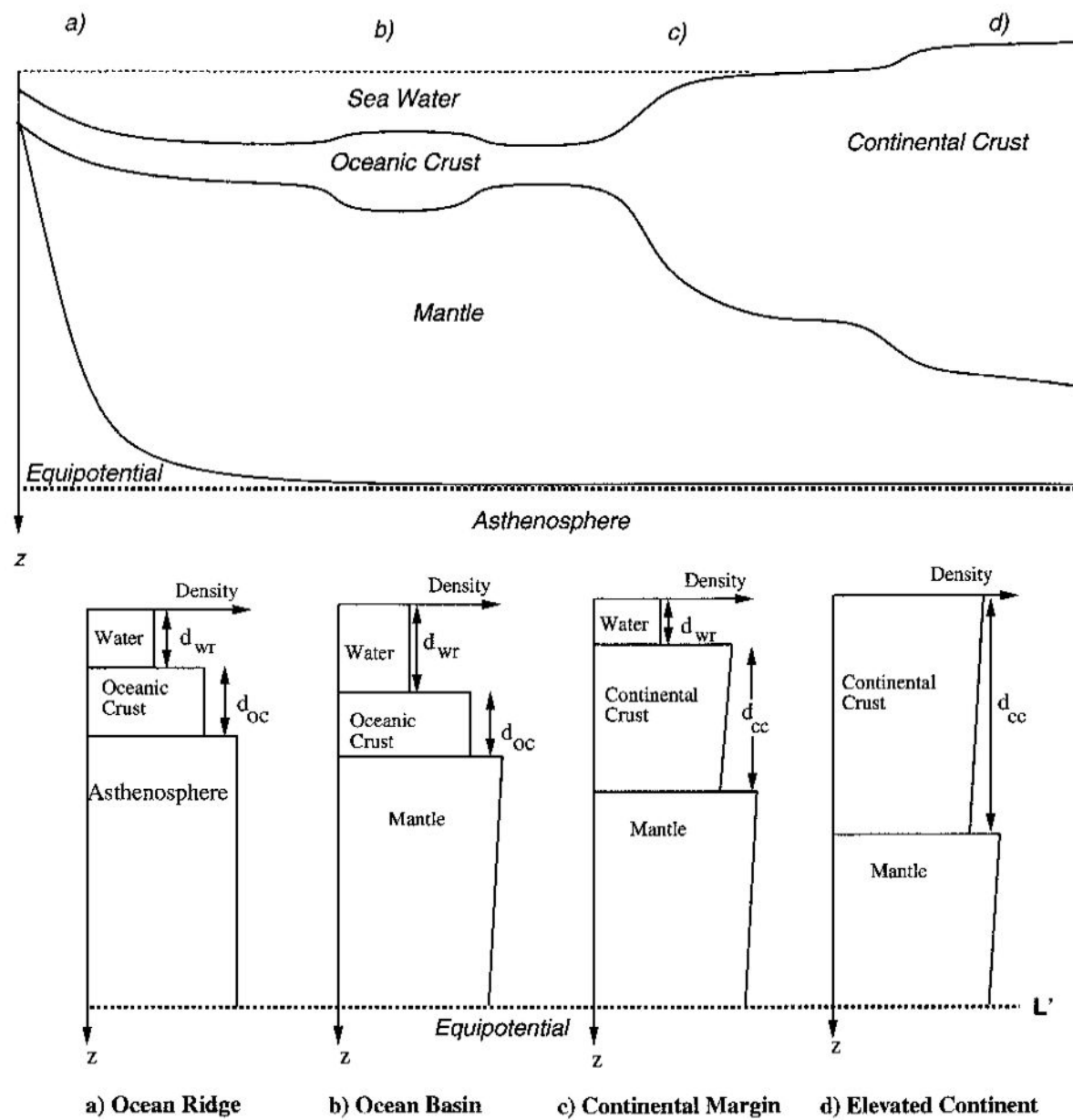


Figure 1. Schematic of the lithospheric depth-density distributions for the four lithospheric types: (a) ocean ridge, (b) oceanic basin, (c) continental margin, and (d) elevated continent. The density of the continental crust and mantle lithosphere varies as a linear function with depth. See text for details.

Table 1. Values of Parameters Used in Calculations

	Definition	Value
T_l	temperature at base of lithosphere	1280°C
T_s	temperature at surface of lithosphere	0°C
h_w	water depth above mid-ocean ridge	2.5 km
h_b	oceanic crust thickness above mid-ocean ridge	7 km
ρ_w	sea water density	1030 kg/m ³
ρ_b	oceanic crust density	2960 kg/m ³
ρ_a	asthenosphere density at T_l	3238 kg/m ³
α_v	coefficient of thermal expansion	$3 \times 10^{-5} \text{ K}^{-1}$
z_l	depth of equipotential surface	125 km

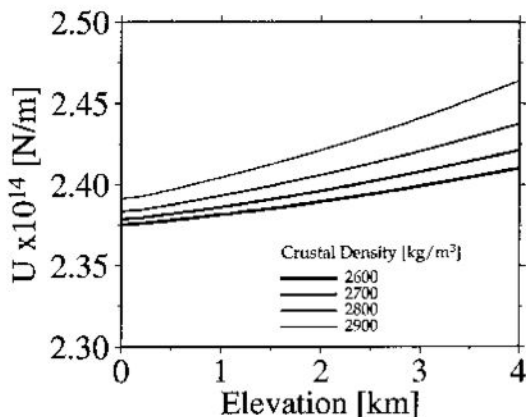


Figure 2. Potential energy of a continental lithosphere column U_l as a function of the assumed crustal density ρ_c ($2600, 2700, 2800$, and 2900 kg m^{-3}) and topography.

The topographic distributions for the Earth and the majority of the continental plates (Africa, Indo-Australia, North America, and South America) are strongly bimodal, reflecting the relative proportion of continents and oceans (continental topography has a mean elevation of several hundred meters, while oceanic bathymetry has a mean depth of about -4 km). The anomalous amount of topography between 0 and 2 km for the African plate reflects the elevated topography associated with the East African rift [Casenave *et al.*, 1989; Anderson, 1989]. The Eurasian, Pacific, and Nazca plates show anomalous topographic distributions. The Eurasian plate is dominated by continent (63%) and continental margin (23%) with very little deep oceanic areas (less than 6%). As a result, the mean elevation for the plate is anomalously high (about 200 m above sea level). In addition, the mean elevation of the continental part of the Eurasian plate is nearly 1 km, reflecting, in part, the influence of the Tibetan plateau topography. While the Pacific and Nazca plates are both oceanic plates, they have significantly different topographic distributions. The Pacific plate is dominated by old, deep basins (50%), while the Nazca plate is principally young, cooling oceanic lithosphere (92%). As discussed below, the varied topographic distributions of the seven major plates is responsible for some significant differences in their respective mean potential energies.

Histograms of U_l for the Earth and the seven major plates are shown in Figure 3b. The varied topographic distributions of the plates produce significant variations in their potential energy distributions. Importantly, the potential energy distributions do not share the distinctive bimodal distribution of topography, due to the fact that for a given surface elevation, ocean lithosphere has much greater potential energy than continental lithosphere. With the exception of the African and Pacific plates, the plate-scale potential energy distributions are characterized by a sharp peak near the mean potential

Table 2. Predicted Geoid Anomaly Across the Continental Margin

$\rho_c, \text{kg m}^{-3}$	N, m
2600	3.3
2700	4.7
2800	6.7
2900	10.0

ρ_c , assumed crustal density; N , predicted geoid anomaly.

energy value \bar{U}_l . The mean potential energies \bar{U}_l for three topographic subsets (all topography, topography below sea level, and topography above sea level) for three values of ρ_c (2700, 2750, and 2800 kg m^{-3}) are listed in Table 4. Table 4 highlights the fact that the potential energy means at both the global and the plate scales are insensitive to the assumed continental crustal density ρ_c . The greatest sensitivity is shown by the Eurasian plate, because of contribution of the elevation related to the Tibetan plateau, with the difference in \bar{U}_l^g for ρ_c of 2700 and 2800 kg m^{-3} , amounting to only $0.6 \times 10^{12} \text{ N m}^{-1}$ (Table 4). For the other four major continental plates the difference in potential energies for this range in ρ_c amounts to $0.2 - 0.4 \times 10^{12} \text{ N m}^{-1}$, while at the global scale the difference is $0.2 \times 10^{12} \text{ N m}^{-1}$.

The principal features of the potential energy distributions can be understood by considering the potential energies associated with the major tectonic features. The potential energy associated with a representative topographic profile which includes each of the four lithospheric types is shown in Figure 4. Also shown in Figure 4 are the mean elevation of the global topography, the mean global potential energy ($\bar{U}_l^g = 2.379 \times 10^{14} \text{ N m}^{-1}$) and the potential energy of the mid-ocean ridge ($U_l^{\text{MOR}} = 2.391 \times 10^{14} \text{ N m}^{-1}$). Note that the mid-ocean ridges and regions of the continents with significant elevated topography have potential energies greater than the global mean, while the oceanic basins are potential energy lows. Table 5 shows that for the range $\rho_c = 2800 - 2700 \text{ kg m}^{-3}$, continental lithosphere with a surface elevation in the range 940–1650 m has the same potential energy as the mid-ocean ridge. The global mean potential energy is equal to the potential energy of cooling oceanic lithosphere at a depth of about 1.3 km and to continental lithosphere with about 70 m elevation (for $\rho_c = 2750 \text{ kg m}^{-3}$, see Table 5). The unimodal potential energy distributions of the major plates reflect this similarity in the potential energy of cooling oceanic lithosphere and near sea level continental lithosphere. The sharp peak in the potential energy distribution for the Pacific plate near $2.36 \times 10^{14} \text{ N m}^{-1}$ reflects the large amount of deep ocean basin in the plate.

In general, the mean potential energy of the continental plates \bar{U}_l^p is very close to \bar{U}_l^g , with the range in

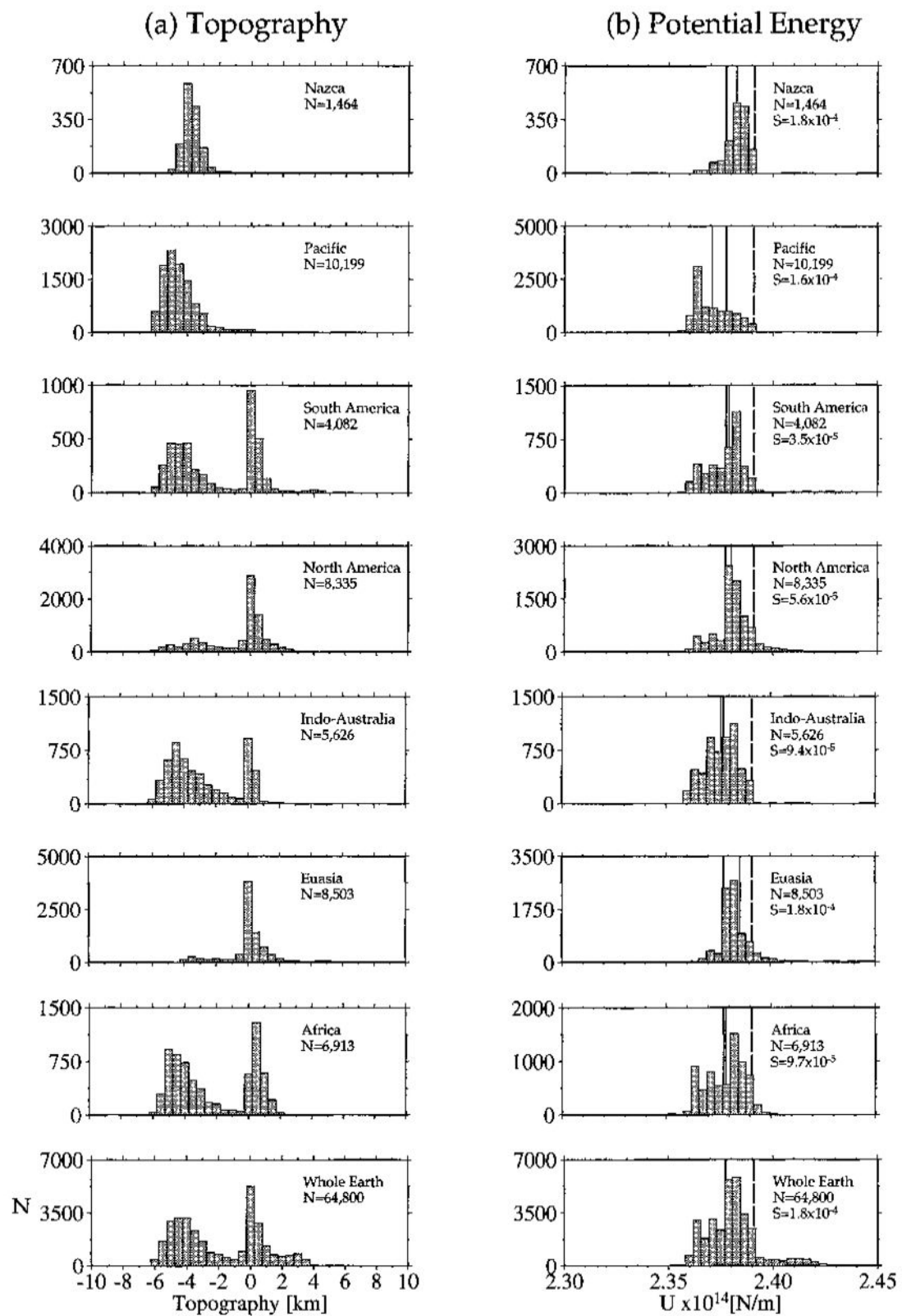


Figure 3. (a) Histograms of the topography and bathymetry for the Earth and the seven major plates. The number of elements (N) for each histogram is also shown. Bin width is 500 m. Diagrams are based on $1^\circ \times 1^\circ$ global topography (ETOPO5). (b) Histograms of the potential energy U_i for the Earth and the seven major plates. Bin width is $1 \times 10^{-11} \text{ N m}^{-1}$. U_i was calculated as described in the text. Dashed vertical lines designate the potential energy of the mid-ocean ridges U_i^{MOR} ($2.391 \times 10^{14} \text{ N m}^{-1}$). Thick solid lines designate the global potential mean U_i^g ($2.379 \times 10^{14} \text{ N m}^{-1}$). Thin solid lines designate the potential mean of the individual plates.

Table 3. Topographic Distribution and Percentage of the Four Principal Lithospheric Types of the Earth and the Seven Major Plates

Plate	Area, $\times 10^7 \text{ km}^2$	\bar{z} , m	\bar{z} , m	\bar{z}^+ , m	YO, %	OO, %	CM, %	C, %
Whole Earth	50.85	-2436	-3647	836	26.0	31.5	14.4	28.1
Africa	7.78	-2152	-3884	650	32.6	21.1	8.1	38.2
Eurasia	6.12	266	-1041	902	1.3	4.5	26.9	67.3
Indo-Australia	6.13	-2768	-3524	339	42.6	19.5	18.4	19.6
North America	5.29	-1000	-2409	658	12.5	14.5	27.0	45.9
South America	4.37	-2059	-3755	608	34.7	15.9	10.6	38.9
Pacific	10.78	-4499	-4520	354	50.2	44.9	4.5	0.4
Nazca	1.66	-3752	-3752	/nodata	92.1	5.0	2.8	0.0

Abbreviations include \bar{z} , average topography; \bar{z}^- , average of topography below sea level; \bar{z}^+ , average of topography above sea level; YO, young oceanic lithosphere; OO, old oceanic lithosphere; CM, continental margin; C, exposed continent.

\bar{U}_l^P for all plates being only $1.2 \times 10^{12} \text{ N m}^{-1}$. The anomalously high mean for the Eurasian plate ($\bar{U}_l^P = 2.383 \times 10^{14} \text{ N m}^{-1}$) is due to the high topography of the Tibetan plateau (where U_l attains values of up to $2.472 \times 10^{14} \text{ N m}^{-1}$), and the mean calculated without this contribution is consistent with the means of other continental plates. The mean for the Indo-Australia plate ($\bar{U}_l^P = 2.375 \times 10^{14} \text{ N m}^{-1}$) is slightly lower than the other continental plates, due to its relatively large proportion of oceanic surface area (60%). The means of the subsets of the continental plates incorporating only those regions exposed above sea level (see Table 4) is substantially greater than \bar{U}_l^P but, importantly, is still less than the potential energy of the mid-ocean ridge.

The oceanic plates, represented by the Pacific and the Nazca plates, have significantly different mean potential energies. The mean for the Pacific plate ($\bar{U}_l^P = 2.371 \times 10^{14} \text{ N m}^{-1}$), which is dominated by old oceanic lithosphere, is much lower than \bar{U}_l^P . In contrast, the mean for the Nazca plate ($\bar{U}_l^P = 2.382 \times 10^{14} \text{ N m}^{-1}$), which is dominated by young oceanic lithosphere, is much greater than \bar{U}_l^P . Thus on the global scale the

mean potential energy of the Pacific and Nazca plates are anomalously low and high, respectively.

Discussion and Conclusions

We have demonstrated the important correlation between potential energy variations and major topographic features of the Earth. The oceanic ridges are features with an excess potential energy ΔU_l ($= U_l - \bar{U}_l^P$) of about $1.2 \times 10^{12} \text{ N m}^{-1}$. Passive continental margins and the ocean basins are features with potential energy less than the global mean, with ΔU_l of 0 to $-1.0 \times 10^{12} \text{ N m}^{-1}$ and $-1.4 \times 10^{12} \text{ N m}^{-1}$, respectively. We note that the magnitude of the potential energy of continental lithosphere with elevated topography is particularly sensitive to the assumed crustal density, and thus quantitative estimates of the excess potential energy of regions with high topography are significantly less robust than our estimates of the mean potential energy at the plate and global scale. For a reference continental crustal density of 2750 kg m^{-3} the global range in potential energy estimated at the $1^\circ \times 1^\circ$ scale is estimated to be about $11 \times 10^{12} \text{ N m}^{-1}$, with the high corre-

Table 4. Mean Potential Energy \bar{U} of the Earth and the Seven Major Plates for Three Assumed Crustal Density Values

Plate	$\bar{U}_{1,\text{all}}^*$	$\bar{U}_{1,-}^*$	$\bar{U}_{1,+}^*$	$\bar{U}_{1,\text{all}}^t$	$\bar{U}_{1,-}^t$	$\bar{U}_{1,+}^t$	$\bar{U}_{1,\text{all}}^t$	$\bar{U}_{1,-}^t$	$\bar{U}_{1,+}^t$
Whole Earth (\bar{U}_l^P)	2.378	2.374	2.386	2.378	2.375	2.389	2.380	2.375	2.392
Africa	2.377	2.373	2.383	2.378	2.374	2.386	2.380	2.374	2.390
Eurasia	2.383	2.375	2.387	2.386	2.377	2.390	2.389	2.379	2.394
Indo-Australia	2.375	2.374	2.381	2.376	2.375	2.383	2.377	2.375	2.386
North America	2.378	2.374	2.384	2.380	2.375	2.386	2.382	2.376	2.390
South America	2.377	2.373	2.384	2.379	2.374	2.386	2.380	2.374	2.390
Pacific	2.371	2.371	2.381	2.371	2.371	2.383	2.371	2.371	2.386
Nazca	2.382	2.382	...	2.382	2.383	...	2.383	2.383	...

Abbreviations include \bar{U}_l , mean potential energies (given in units of 10^{14} N m^{-1}); $\bar{U}_{1,\text{all}}$, all topography; $\bar{U}_{1,-}$, topography below sea level; $\bar{U}_{1,+}$, topography above sea level; \bar{U}_l^P , mean potential energy of the lithosphere.

* Assumed crustal density $\rho_c = 2700 \text{ kg m}^{-3}$.

† Assumed crustal density $\rho_c = 2750 \text{ kg m}^{-3}$.

‡ Assumed crustal density $\rho_c = 2800 \text{ kg m}^{-3}$.

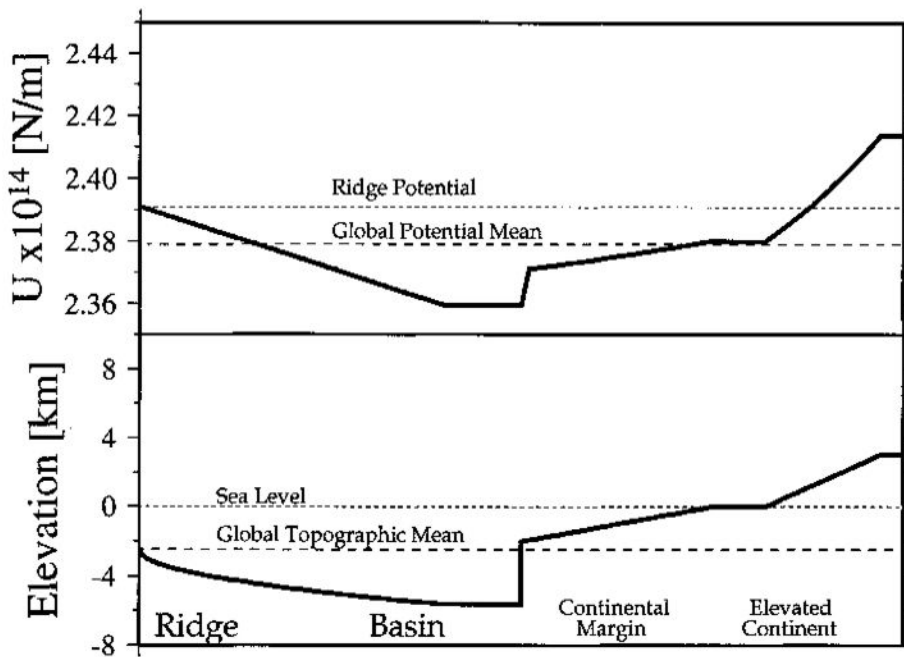


Figure 4. Calculated potential energy U_i across a topographic cross section representing the mid-ocean ridge, oceanic basin, passive (Atlantic-type) continental margin, and elevated continental lithosphere. Also shown are the global topographic mean (-2880 m), ridge potential ($2.391 \times 10^{14} \text{ N m}^{-1}$), and mean global potential energy ($2.379 \times 10^{14} \text{ N m}^{-1}$), calculated with $\rho_c = 2750 \text{ kg m}^{-3}$.

sponding to the highest parts of the Himalaya-Tibetan Plateau system ($U_i = 2.472 \times 10^{14} \text{ N m}^{-1}$ at elevation 6400 m) and the low corresponding to old ocean basin ($U_i = 2.364 \times 10^{14} \text{ N m}^{-1}$). In general, the potential energy means of the continental plates are very close to the global mean.

In order to evaluate the relationship between potential energy variations and continental deformation, it is necessary to assess the strength of the continental lithosphere. Relatively little is known about the absolute strength of the lithosphere and how such strength is distributed with depth [e.g., Zoback *et al.*, 1993]. Laboratory-based strength estimates predict very heterogeneous strength distributions, with discrete strength maxima associated with compositional and rheological stratification within the lithosphere [Brace and Kohlstedt, 1980]. The strength of the lithosphere is dependent on both the lithological constitution and the ther-

mal regime, both of which are known to vary widely. On the basis of such laboratory estimates a number of workers [e.g., Houseman and England, 1986; Kushnir and Park, 1987] have suggested that the extensional strength of the lithosphere at the limit of geologically significant strain rates is of the order of $3-4 \times 10^{12} \text{ N m}^{-1}$. More recently, Kushnir [1992] argued that extensional strength may be considerably reduced, possibly to as little as $2 \times 10^{12} \text{ N m}^{-1}$, due to the visco-elastic amplification of stresses in the lithosphere. Estimates of the upper-crustal strength inferred from stress measurements in the KTB (Continental Deepbore Drilling Program) wellhole in Germany show that the cumulative force needed to deform crustal material is in the range of $2-5 \times 10^{12} \text{ N m}^{-1}$ (Zoback *et al.*, 1993). Although such estimates are highly uncertain, we note that these strength estimates are of the order of the potential-variations predicted in this study.

Table 5. Elevation of Continental Lithosphere in Potential Energy Balance With the Global Mean \bar{U}_i^g and the Mid-Ocean Ridge U_i^{MOR}

$\rho_c, \text{kg m}^{-3}$	\bar{U}_i^g, m	$U_i^{\text{MOR}}, \text{m}$
2800	-160	940
2750	70	1400
2700	220	1650

Abbreviations include \bar{U}_i^g , mean gravitational potential energy; U_i^{MOR} , mean potential energy of mid-ocean ridge; and ρ_c , assumed crustal density.

Potential Energy Torques

The influence of lateral density variations on the lithospheric stress field is proportional to the density moment of the mass dipole formed by the mass anomaly, with positive mass anomalies producing tectonic compression [Fleitout, 1991]. The contribution of potential energy variations within the lithosphere to the total torque acting on the plates was calculated by using the "moment law" in a plane stress finite element analysis. This was accomplished by applying a basal shear force to each element proportional to the horizontal gradient of the local dipole moment (which is proportional to U_1 , see (3) and (4)) [Fleitout, 1991; Richardson and Reding, 1991]. For plane geometry this force can be expressed as

$$L \left(\frac{\partial \sigma_{xx}}{\partial x} + \frac{\partial \sigma_{xy}}{\partial y} \right) = \sigma_{xz}^L - \frac{L \partial M}{\partial x} \quad (9)$$

$$L \left(\frac{\partial \sigma_{yy}}{\partial y} + \frac{\partial \sigma_{xy}}{\partial x} \right) = \sigma_{yz}^L - \frac{L \partial M}{\partial y} \quad (10)$$

where L is the thickness of the lithosphere; M is the density moment; and $\frac{\partial}{\partial x}$ and $\frac{\partial}{\partial y}$ are the partial derivative with respect to x and y , respectively. The resulting torque is calculated as

$$\mathbf{T} = \mathbf{r} \times \mathbf{F} \quad (11)$$

where \mathbf{r} is the radius position vector, and \mathbf{F} is the force acting on the plate. The total torque acting on the plate is found by integrating \mathbf{T} over the surface of the plate.

Calculating the torque acting on the plates owing to potential energy differences provides a way of quantifying the importance of these differences within the plate. The total torque contribution from the potential energy distributions within the plates is plotted in Figure 5 for three cases: (1) mid-ocean ridges alone; (2) topography alone; and (3) all potential energy sources. The total torques and angular misfit between the torque poles and the absolute plate velocity poles [Minster and Jordan, 1978; Gripp and Gordon, 1990] are listed in Table 6. Whereas the mean potential energies of the plates (see Figure 3) are inherently clustered about the global mean potential energy, Figure 5 demonstrates there is significant variation in the relative torque contributions from the potential energy distributions within the individual plates. Torques associated with the mid-ocean ridges exceed $4 \times 10^{25} \text{ N m}^{-1}$ for the plates with a significant amount of mid-ocean ridge (i.e., the North and South American, Nazca, Indo-Australian, and Pacific plates). Torques associated with the continental topography are typically about $2.5 \times 10^{25} \text{ N m}^{-1}$ and are considerably smaller than the ridge torques. The angular misfit between the absolute plate velocity azimuths and the ridge torques is considerably less for plates with large potential energy torques (i.e., less than 25° for the South American, Nazca, Indo-Australian and Pacific plates). The low total ridge torque for the African plate reflects the circular geometry of the plate and the fact that since

the plate is nearly surrounded by mid-ocean ridges, the torque due to the ridge force nearly cancels. The weak correlation between ridge torques and plate velocities was originally pointed out by Forsyth and Uyeda [1975]. There is little correlation between the topography torques and the absolute plate velocities. Furthermore, the angular misfit between the torque and velocity poles is very large for the topography torques, in excess of 90° for most of the plates. While topographic forces are certainly an important sources of stress, it is clear that mid-ocean ridge torques play a more important role in the plate-scale dynamics. This observation supports the notion that ridge push forces are an important component of the driving mechanism and global intraplate deformation [Richardson, 1992]. The strong correlation between the potential energy distributions and plate velocities, at least for the fast moving plates, supports the argument that the absolute reference frame is determined by the surface plates themselves rather than sublithospheric flow.

In order to facilitate the comparison between the torque directions and plate motions for plates with small velocities and torques, the vectors have been normalized to unit length in Figure 6. In Figure 7 the length of the vectors reflects the absolute magnitudes. As discussed by Richardson [1992], there is a very strong correlation between the ridge torque directions and the azimuth of the absolute plate velocities. This is particularly true for the North American, South American, Pacific, and Indo-Australian plates. Large topography torques exist in the Eurasian, Indo-Australian, North American, and South American plates. In contrast to the ridge torque directions, the topography torques act at a large angle to the plate motion directions. In the case of the total potential energy torques, there is a strong correlation between the torque directions and the azimuths of the absolute plate velocities. The relationship between the torque directions and the plate motions demonstrates that while topographic forces are certainly an important sources of stress, mid-ocean ridge torques would seem to play a more important role in the plate-scale dynamics.

Tectonic Reference State

The concept of a tectonic reference state (TRS) has proved useful in evaluating the contribution of lateral density variations to the intraplate stress field [e.g., Zhou and Sandiford, 1992]. In general, a lithospheric column in potential and isostatic balance with the TRS will remain undeformed in the absence of external forces. A number of studies of continental deformation have used the concept of the TRS to illustrate the importance of potential energy (or buoyancy forces) changes which accompany lithospheric deformation [e.g., Houseman and England, 1986; Sonder et al., 1987; England and Houseman, 1988, 1989; Zhou and Sandiford, 1992].

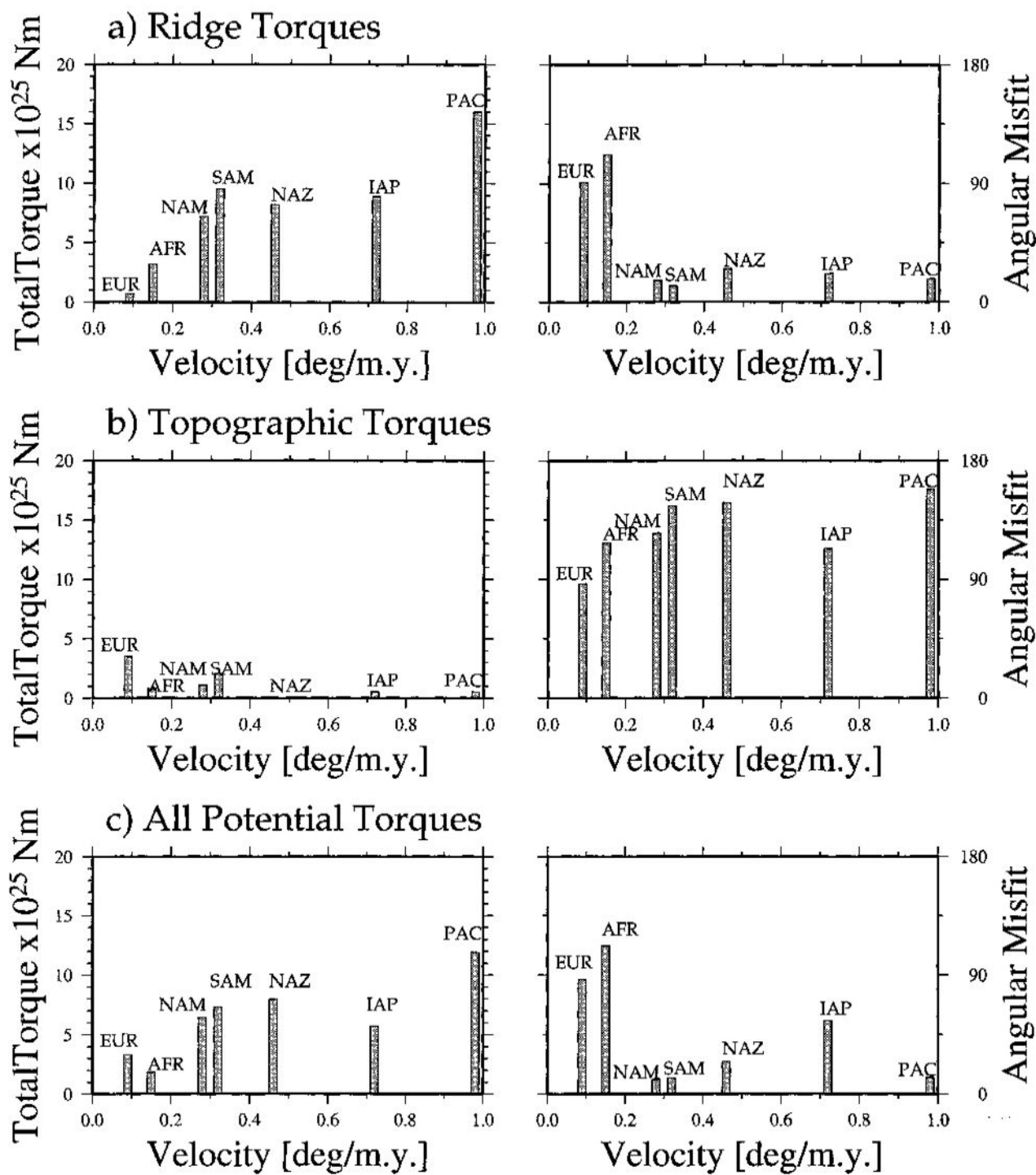


Figure 5. Total torque versus absolute plate velocity for potential energy differences due to (a) mid-ocean ridges, (b) topography, and (c) all potential energy sources. Also shown are the angular misfit between the torque poles (listed in Table 6) and the absolute plate velocity poles. Plate velocity information is from *Minster and Jordan* [1978] for the Indo-Australian plate and from NUVEL-1 [*Gripp and Gordan*, 1990] for all other plates. Plate abbreviations are EUR, European; AFR, African; NAM, North American; SAM, South American; NAZ, Nazca; IND, Indo-Australian; PAC, Pacific.

As discussed above, the TRS is best defined in terms of the potential energy distributions at either the plate or global scale, which can be characterized by $\overline{U_l^P}$ and $\overline{U_l^G}$, respectively. This study has shown, however, that the

continental plates (with the exception of the Eurasian plate) have mean potential energies $\overline{U_l^P}$ close to the global mean $\overline{U_l^G}$. Moreover, if the contribution of the Tibetan Plateau is excluded, this relationship also holds

Table 6. Torques Due to Mid-Ocean Ridges, Topography, All Potential Energy Sources, and Angular Misfit Information

Plate	Magnitude, $\times 10^{25}$ N m	Latitude, deg N	Longitude, deg E	Angular Misfit, deg
<i>Mid-Ocean Ridge</i>				
PAC	16.0	-77.5	94.5	17.4
NAM	7.2	-60.2	-43.9	15.9
SAM	9.5	-68.0	109.1	12.3
EUA	0.7	-44.5	-128.3	90.5
AFR	3.2	57.9	-34.4	111.6
IND	8.9	40.0	30.1	21.3
ANT	5.8	-38.8	158.9	83.1
NAZ	8.2	64.2	-120.4	24.9
COC	1.0	64.4	149.0	75.6
CAR	0.7	52.6	-176.9	169.2
ARB	0.2	31.8	161.0	119.6
PHL
<i>Topography</i>				
PAC	0.5	57.3	-132.0	158.4
NAM	1.1	38.3	79.1	125.0
SAM	2.1	22.1	17.6	145.9
EUA	3.5	6.5	-20.6	86.7
AFR	0.8	-16.8	-74.2	117.6
IND	0.5	-39.3	109.8	90.5
ANT	0.4	-3.4	-178.5	113.7
NAZ	0.3	-63.1	41.1	147.9
COC
CAR	0.2	33.2	0.1	95.8
ARB	0.9	-25.4	117.5	105.2
PHL
<i>All Potential Energy Sources</i>				
PAC	11.9	-72.6	87.7	12.5
NAM	6.4	-60.1	-30.0	10.9
SAM	7.3	-58.2	-72.0	12.2
EUA	3.3	-1.8	-29.0	86.7
AFR	1.8	20.3	-67.0	112.1
IND	5.7	53.2	93.4	55.7
ANT	6.1	-36.9	160.6	84.8
NAZ	7.9	64.2	-119.7	24.7
COC	1.0	64.4	148.9	75.6
CAR	0.7	66.0	-175.4	174.3
ARB	1.1	-16.6	124.7	109.9
PHL	0.8	56.7	-94.7	122.8

Angular misfit between the torque poles and the absolute plate velocities poles is based on plate velocity information from *Minster and Jordan* [1978] for the Indo-Australian plate and NUVEL-1 [*Gripp and Gordon*, 1990] for all other plates. Plate abbreviations are PAC, Pacific; NAM, North American; SAM, South American; EUA, European; AFR, African; IND, Indo-Australian; ANT, Antarctic; NAZ, Nazca; COC, Cocos; CAR, Caribbean; ARB, Arabian; PHL, Philippine.

true for the Eurasian plate. Thus as far as continental tectonics is concerned, it would appear to make little functional difference whether the TRS is defined by a column in potential energy balance with the global or individual-plate mean. The mean global potential energy corresponds to the potential energy of continental lithosphere of near sea level elevation, as well as cooling oceanic lithosphere at a depth of about 4.3 km

below sea level. Therefore it is self-consistent to use sea level continental lithosphere as the TRS for evaluating continental deformation. The definition of the continental TRS proposed here contrasts with that of a number of previous studies which assumed a reference state in potential energy balance with mid-ocean ridges [*Turcotte et al.*, 1977; *McKenzie*, 1978; *Le Pichon and Angelier*, 1979; *Cochran*, 1982; *Le Pichon*, 1983;

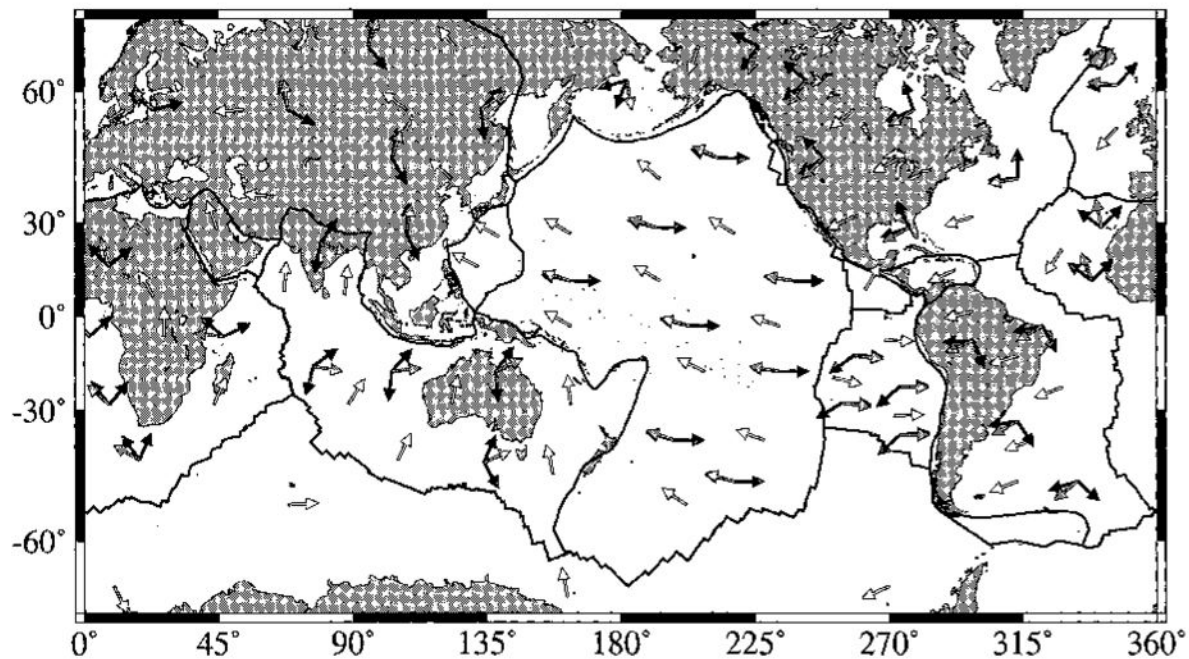


Figure 6. Comparison of ridge torque (solid arrows), topographic torque (medium gray shaded arrows), total potential energy torque (light gray shaded arrows), and absolute velocity directions (open arrows) for the seven major plates. The magnitude of the torques and velocity vectors have been normalized to unit length. Plate velocity information is from *Minster and Jordan [1978]* for the Indo-Australian plate and from NUVEL-1 [*Gripp and Gordan, 1990*] for all other plates. The Pacific ridge and total torque arrows nearly coincide because the total torque acting on the plate is dominated by the ridge torque.

Absolute

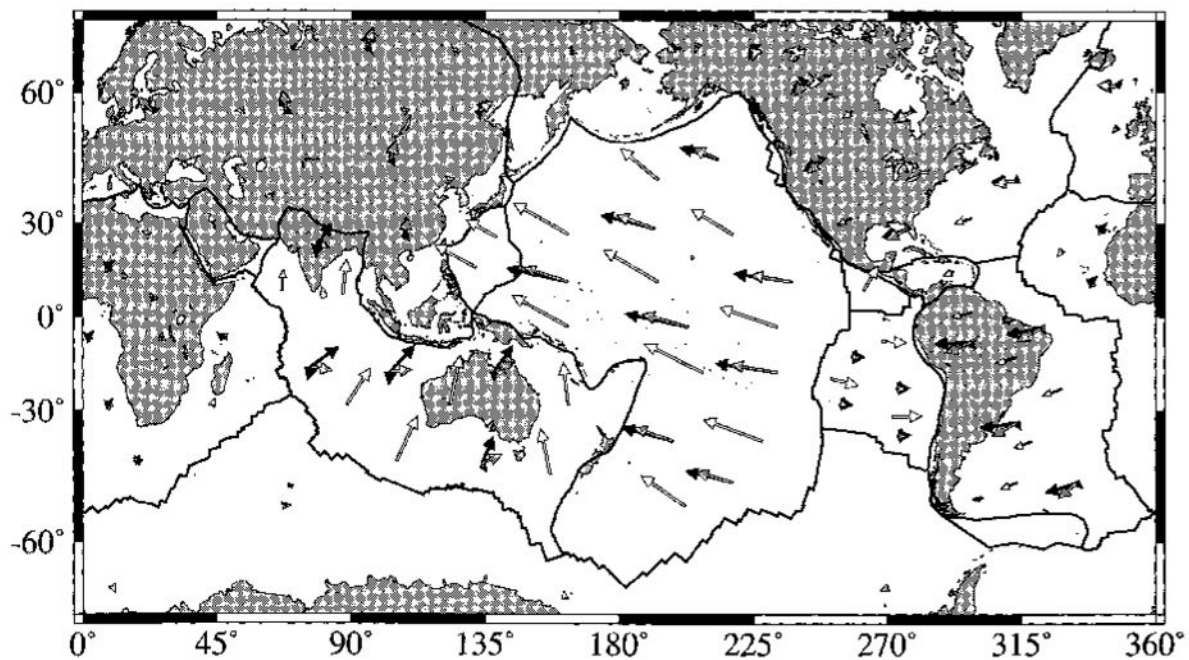


Figure 7. Comparison of ridge torque (solid arrows), topographic torque (medium gray shaded arrows), total potential energy torque (light gray shaded arrows), and absolute velocity directions (open arrows) for the seven major plates. The length of the vectors reflects the absolute magnitude of the torques and velocities. The Pacific ridge and total torque arrows nearly coincide because the total torque acting on the plate is dominated by the ridge torque. See Figure 5 for other details. The lengths of the arrows reflect the absolute magnitude of the torques.

[Turcotte, 1983; Crough, 1983; Houseman and England, 1986; England and Houseman, 1988, 1989; Sonder et al., 1987; Zhou and Sandiford, 1992]. The difference in definitions amounts to about $1.2 \times 10^{12} \text{ N m}^{-1}$. Some uncertainty in these calculations is obviously introduced by our inadequate knowledge of the density structure of the lithosphere. While independent constraints from the geoid anomalies associated with continental margins provide a way to estimate the mean density of the continental crust, it remains the least constrained parameter. However, it has been shown that the global and plate mean potential energies are insensitive to the assumed continental crustal density. Thus this definition of the TRS can be considered to be robust.

Ambient Stress State

The intraplate stress field in slow moving plates which are surrounded by mid-ocean ridges may be expected to approximate the ambient stress state [Crough, 1983]. For the first-order potential energy distribution considered in this study, regions of tectonic tension and compression can be related to the difference between the potential energy of a lithospheric column and the TRS. We note that this may not be true for the stress state in the case where there is significant variation in the mechanical strength of the lithosphere [e.g., Fleitout and Froidevaux, 1982, 1983]. Such effects can be considered as second-order and are not addressed in this study. We have shown that the potential energy of the mid-ocean ridges is in excess of the mean plate potential energy with the difference ΔU_l approximately equal to $1.2 \times 10^{12} \text{ N m}^{-1}$ for plates containing a large amount of continental lithosphere. Consequently, in the ambient state the ridges and much of the ridge flanks can be expected to exhibit an extensional stress regime with the maximum horizontal compressive stress direction $S_{H,\max}$ oriented parallel to the ridge axis. Correspondingly, the direction of maximum tension will be aligned with the gradient in potential energy and hence with the gradient in bathymetry. The difference between the potential energy of the mid-ocean ridges and the global mean can be used to constrain the contribution of the ridge push force to the intraplate stress field. Although the ridges have an excess potential energy over the old ocean basins of about $2.6 \times 10^{12} \text{ N m}^{-1}$, the compressional force witnessed by old ocean basin lithosphere in the ambient state must be somewhat less, since it reflects the potential energy difference relative to the plate mean (that is, ΔU_l which is about $-1.4 \times 10^{12} \text{ N m}^{-1}$ for old ocean basin) and not relative to the ridge. Similarly, while the ridges have potential energy in excess of much of the continental mass with low elevations, it is potential energy relative to the plate mean (and not the ridges) that dictates the ambient stress state in the continents. The implication is that for reference continental crustal densities in the range of 2750 kg

m^{-3} the ambient stress state in the exposed continental mass should be extensional (or strike slip). Because large regions of compression are thought to be the dominate state of stress in most of the continental plates, particularly in eastern North America and western Europe [Zoback and Magee, 1991; Zoback et al., 1992], this conclusion suggests that other sources of tectonic stress (i.e., plate boundary forces) play an important role in the nature of intraplate stress field in these nonambient plates.

Appendix A

In this appendix we present the closed-form solutions for the potential energy for each of the lithospheric types, subject to the constraints outlined in the text.

For young oceanic lithosphere the potential energy is given by

$$\begin{aligned} \frac{U_l}{g \rho_m z_l^2} = & \frac{3 + 2\omega}{6} + (-1 + \delta)(1 + \omega)\psi \\ & + \frac{(1 - \delta)(1 + 2\omega)\psi^2}{2} \\ & + \frac{(3 + 2\omega - 3\psi + 3\delta\psi)\psi_1}{3} \\ & - \frac{(3\omega\psi + 3\delta\omega\psi)\psi_1}{3} \\ & + \frac{(3 + 2\omega)\psi_1^2}{6} \\ & + \frac{-(\omega\psi^3) + \delta\omega\psi^3}{3(1 + \psi_1)} \end{aligned} \quad (\text{A1})$$

For old oceanic lithosphere the potential energy is given

by

$$\begin{aligned} \frac{U_l}{g \rho_m z_l^2} = & \frac{3 + 2\omega}{6} + (-1 + \delta)(1 + \omega)\psi \\ & + \frac{(1 - \delta)(1 + 2\omega)\psi^2}{2} \\ & + \frac{(3 + 2\omega - 3\psi + 3\delta\psi)\psi_1}{3} \\ & - \frac{(3\omega\psi + 3\delta\omega\psi - 3\delta_2)\psi_1}{3} \\ & + \frac{(3 + 2\omega - 3\delta_2)\psi_1^2}{6} \\ & + \frac{-(\omega\psi^3) + \delta\omega\psi^3}{3(1 + \psi_1)} \end{aligned} \quad (\text{A2})$$

For submerged continental marginal lithosphere the potential energy is given by

$$\begin{aligned} \frac{U_l}{g \rho_m z_l^2} = & \frac{1}{2} + (-\omega + \delta_1 - \delta_2) \psi_1 \\ & + \frac{(-\omega + \delta_1 - \delta_2) \psi_1^2}{2} \\ & + \frac{3\omega \psi_1^2 + \omega \psi_1^3}{6 \psi_3} + \frac{\omega (1 + \psi_1) \psi_3}{2} \\ & - \frac{\omega \psi_3^2}{6} \end{aligned} \quad (\text{A3})$$

For exposed continental lithosphere the potential energy is given by

$$\begin{aligned} \frac{U_l}{g \rho_m z_l^2} = & \frac{1}{6} + \frac{(1 - \delta)(1 + 2\omega) \psi^2}{2} \\ & + \frac{(3 + 2\omega - 3\psi + 3\delta\psi) \psi_1}{3} \\ & + \frac{(3 + 2\omega - 3\delta_2) \psi_1^2}{6} \\ & + \frac{-(\omega \psi^3) + \delta \omega \psi^3}{3(1 + \psi_1)} \end{aligned} \quad (\text{A4})$$

where the denoted parameters are defined as

$$\omega = \alpha T_l; \psi = \frac{z_c}{z_{\text{iso}}}$$

$$\psi_1 = \frac{h}{z_{\text{iso}}}; \psi_2 = \frac{z_w}{z_{\text{iso}}}$$

$$\psi_3 = \frac{z_l}{z_{\text{iso}}}; \delta = \frac{\rho_c}{\rho_m}$$

$$\delta_1 = \frac{\rho_b}{\rho_m}; \delta_2 = \frac{\rho_w}{\rho_m}$$

In these expressions, h is the surface topography (above sea level), z_w is the bathymetry, z_{iso} is the depth of isostatic compensation (beneath sea level), z_c is the crustal thickness (see below), z_l is the lithospheric thickness, and ρ_c , ρ_m , and ρ_w are the crustal, mantle, and seawater densities, respectively.

We use topography as the basic constraint and calculate the crustal thickness for continents and old ocean basin assuming the base of the lithosphere is at depth z_{iso} . For exposed continental lithosphere the crustal thickness is given by

$$\begin{aligned} z_c = & z_1 \theta - \frac{1}{\alpha \sqrt{\Delta \rho_1} T_l} \\ & x [z_1^2 \Delta \rho_1 + 2\beta z_1 (h_0 \rho_b - h \rho_c) \\ & - h_0 \rho_m - h_w \rho_m \\ & - h_w \rho_w z l_0 \Delta \rho_1] - \beta^2 \rho_c z_1]^{1/2} \end{aligned} \quad (\text{A5})$$

The crustal thickness for submerged continental marginal lithosphere (continental margin) is calculated as

$$\begin{aligned} z_{cm} = & z_1 \theta - \frac{1}{\alpha \sqrt{\Delta \rho_1} T_l} \\ & x [z_1^2 \Delta \rho_1 + 2\beta z_1 (h_0 \rho_b - h \rho_c) \\ & - h_0 \rho_m - h_w \rho_m - h_w \rho_w \\ & + h \rho_w z l_0 \Delta \rho_1] - \beta^2 \rho_c z_1]^{1/2} \end{aligned} \quad (\text{A6})$$

In old oceanic lithosphere, crustal thickness for anomalous topography is calculated as

$$\begin{aligned} z_{ob} = & z_1 \theta - \frac{1}{\alpha \sqrt{\Delta \rho_2} T_l} \\ & x [z_1^2 \Delta \rho_2 + 2\beta z_1 (h_0 \rho_b - h \rho_b \\ & - h_0 \rho_m - h_w \rho_m - h_w \rho_w \\ & + h \rho_w z l_0 \Delta \rho_2) - \beta^2 \rho_b z_1]^{1/2} \end{aligned} \quad (\text{A7})$$

In young oceanic lithosphere the thickness for the cooling oceanic lithosphere is calculated assuming constant ocean crustal thickness as follows:

$$z_{lp} = \frac{h_0 z}{\beta} \left(\frac{\rho_w}{\rho_m} - 1 \right) - \frac{z \Delta \rho_2}{\rho_m} \sqrt{1 + \frac{2\beta h_0 \rho_m}{z \Delta \rho_2}} \quad (\text{A8})$$

In these expressions

$$\Delta \rho_1 = (\rho_m - \rho_c)$$

$$\Delta \rho_2 = (\rho_m - \rho_b)$$

$$\beta = \alpha T_l$$

$$z_1 = (h + z l_0)$$

$$\theta = \left(1 + \frac{1}{\beta} \right)$$

Appendix B

We make the assumption that regions of elevated topography in the continents are supported mainly by thickened crust calculated on the assumption that the base of the continental lithosphere is everywhere at a constant depth corresponding to $z_{\text{iso}} = 125$ km. In many regions of the continents, elevated topography is likely to be supported by thinned mantle lithosphere, with or without thickened crust. In order to evaluate the errors in the potential energy calculations introduced by this approximation, the approach of *Sandiford and Powell* [1990] is adopted. In this case, the difference in potential energy of two lithospheric column in isostatic equilibrium (subject to the constraints adopted in this paper, i.e., no internal heat production) can be approximated by

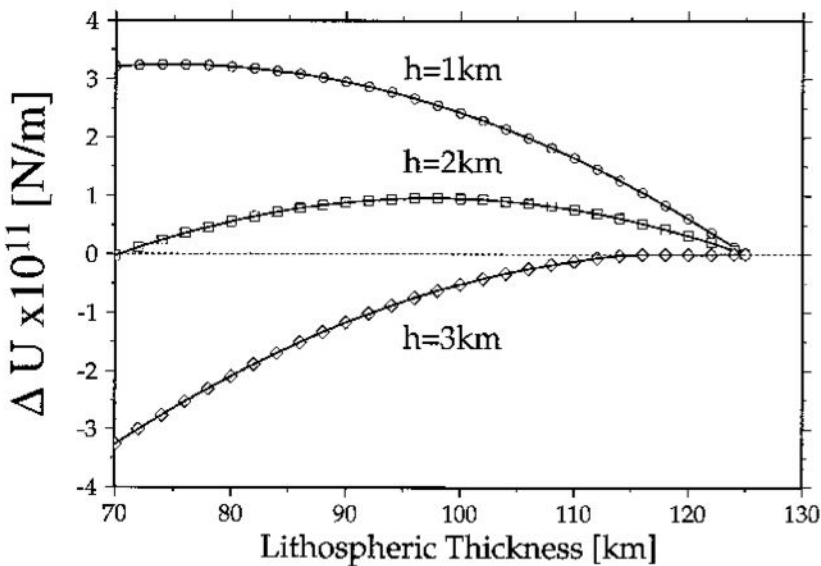


Fig. B1. Potential energy of a lithospheric column with thinned lithosphere relative to a reference lithosphere, $\Delta U_h = U|_{z_1=z} - U|_{z_1=125\text{ km}}$ for three values of surface elevation h of 1, 2, and 3 km.

$$\begin{aligned} \frac{\Delta U}{g \rho_m z_c^2} &= \delta \frac{(1-\delta)}{2} (f_c^2 - 1) \\ &\quad - \frac{\alpha T_l}{6 \psi^2} [f_l^2 - 1 - 3(1-\delta)(f_c f_l - 1)] \\ &\quad - \frac{\alpha^2 T_l^2}{8 \psi^2} (f_l^2 - 1) \end{aligned} \quad (\text{B1})$$

where f_c and f_l are the ratios of the thickness of the crust and whole lithosphere for the two columns (taken relative to the reference column against which the potential energy difference is to be measured); ψ is the ratio of crustal to whole lithospheric thickness in the reference column; and z_c is the thickness of the crust in the reference column (in this formulation the approximation that $\alpha \rho_c = \alpha \rho_m$ was used). In order to evaluate the effect of the isostatic support mechanism, we compare the potential energy difference ΔU_h between a lithospheric column with thinned lithosphere and a reference lithosphere with a base at $z_{\text{iso}} = 125$ km

$$\Delta U_h = U|_{z_1=z} - U|_{z_1=125\text{ km}} \quad (\text{B2})$$

with the results for elevations in the range $h = 1000 - 3000$ m shown in Figure B1. For this topographic range the errors in the calculated potential energy introduced by assuming isostatic support by thickened crust are no greater than about 3×10^{11} N m⁻¹. It is therefore reasonable to conclude that in this range of topography the potential energy of the lithospheric columns is insensitive to nature of the isostatic support mechanism.

Acknowledgments. This work was partially funded through funds made available by the Australian Petroleum Cooperative Research Centre as part of a study of the factors controlling the intraplate stress field along the Northwest Shelf of Australia. We are greatly indebted to our colleagues working on this project, Richard Hillis and Shaohua Zhou, for their encouragement and suggestions. An anonymous reviewer is thanked for thorough comments made on an earlier version of this manuscript. Southern Arizona Seismic Observatory contribution No. 28.

References

- Anderson, D. L., *Theory of the Earth*, 366 pp., Blackwell, Oxford, 1989.
- Artyushkov, E. V., Stresses in the lithosphere caused by crustal thickness inhomogeneities, *J. Geophys. Res.*, **78**, 7675-7708, 1973.
- Cazenave, A., A. Souriau, and K. Dominh, Global coupling of Earth surface topography with hotspots, geoid and mantle heterogeneities, *Nature*, **340**, 54-57, 1989.
- Coblenz, D. D., and R. M. Richardson, Constraints on continental margin dynamics from GEOSAT ERM data (abstract), *EOS Trans. AGU, Fall Meeting Suppl.*, **73**, 571, 1992.
- Cochran, J. R., The magnetic quiet zone in the eastern Gulf of Aden: Implications for the early development of the continental margin, *Geophys. J. R. Astron. Soc.*, **68**, 171-202, 1982.
- Crough, S. T., Rifts and swells: Geophysical constraints on causality, *Tectonophysics*, **94**, 23-37, 1983.
- Dahlen, F. A., Isostacy and the ambient state of stress in the oceanic lithosphere, *J. Geophys. Res.*, **86**, 7801-7807, 1981.
- England, P. C., Diffuse deformation: Length scales, rates and metamorphic evolution, *Philos. Trans. R. Soc. London A*, **321**, 3-22, 1987.
- England, P. C., and G. A. Houseman, The mechanics of the Tibetan Plateau, *Philos. Trans. R. Soc. London A*, **326**, 301-319, 1988.
- England, P. C., and G. A. Houseman, Extension during continental convergence, with application to the Tibetan Plateau, *J. Geophys. Res.*, **94**, 17,561-17,579, 1989.
- England, P. C., and D. McKenzie, A thin viscous sheet model of continental deformation, *Geophys. J. R. Astron. Soc.*, **70**, 295-321, 1982.
- England, P. C., and P. Molnar, Inferences of deviatoric stress in actively deforming belts from simple physical models, *Philos. Trans. R. Soc. London A*, **337**, 151-164, 1991.
- Fleitout, L., The sources of lithospheric tectonic stresses, *Philos. Trans. R. Soc. London A*, **337**, 73-81, 1991.
- Fleitout, L., and C. Froidevaux, Tectonics

- and topography for a lithosphere containing density heterogeneities, *Tectonics*, 1, 21-56, 1982.
- Fleitout, L., and C. Froidevaux, Tectonic stresses in the lithosphere, *Tectonics*, 2, 315-324, 1983.
- Forsyth, D., and S. Uyeda, On the relative importance of the driving forces of plate motion, *Geophys. J. R. Astron. Soc.*, 48, 163-200, 1975.
- Frank, F. C., Plate tectonics, the analogy with glacier flow and isostasy, Flow and Fracture of Rocks, *Geophys. Monogr. Ser.*, vol. 16, edited by H. C. Heard et al., pp. 285-292, AGU, Washington, D.C., 1972.
- Gripp, A. E., and R. G. Gordon, Current plate velocities relative to the hotspots incorporating the NUVEL-1 global plate motion model, *Geophys. Res. Lett.*, 17, 1109-1112, 1990.
- Haxby, W. F., and D. L. Turcotte, On isostatic geoid anomalies, *J. Geophys. Res.*, 83, 5473-5478, 1978.
- Houseman, G., and P. England, A dynamical model of lithosphere extension and sedimentary basin formation, *J. Geophys. Res.*, 91, 719-729, 1986.
- Houseman, G., D. McKenzie, and P. Molnar, Convective instability of a thickened boundary layer and its relevance for the thermal evolution of continental convergence zones, *J. Geophys. Res.*, 86, 6115-6132, 1981.
- Kaula, W. M., Earth's gravity field: Relation to global tectonics, *Science*, 169, 982-985, 1970.
- Kaula, W. M., Global gravity and tectonics, in *The Nature of the Solid Earth*, edited by E.C. Robertson, pp. 385-405, McGraw-Hill, New York, 1972.
- Kushnir, N., The distribution of stress with depth in the lithosphere: thermorheological and geodynamic constraints, in *Tectonic stress in the lithosphere* edited by R.B. Whitmarsh, M.H.P. Bott, J.D. Fairhead, and N.J. Kuszmir, pp. 95-110, *The Royal Society of London*, 1991.
- Kushnir, N., and R. Park, The extensional strength of the continental lithosphere: its dependence on geothermal gradient and crustal composition and thickness, in *Continental Extensional Tectonics* edited by M. P. Coward, J. F. Dewey, and P. L. Hancock, *Geol. Soc. Spec. Publ. London*, 28, 35-52, 1987.
- Le Pichon, X., Land-locked oceanic basins and continental collision: The eastern Mediterranean as a case example, in *Mountain Building Processes*, edited by K. J. Hsue, pp. 201-211, Academic, San Diego, Calif., 1983.
- Le Pichon, X., and J. Angelier, The Hellenic arc and trench system: A key to the neotectonic evolution of the eastern Mediterranean area, *Tectonophysics*, 60, 1-42, 1979.
- Lister, C. R., Gravitational drive on oceanic plates caused by thermal contraction, *Nature*, 257, 663-665, 1975.
- McKenzie, D. P., Active tectonics of the Alpine-Himalayan belt: The Aegean sea and surrounding regions, *Geophys. J. R. Astron. Soc.*, 55, 217-254, 1978.
- Molnar, P., and H. Lyon-Caen, Some simple physical aspects of the support, structure, and evolution of mountain belts, *Spec. Pap. Geol. Soc. Am.*, 218, 179-207, 1988.
- Molnar, P., and P. Tapponier, Active tectonics of Tibet, *J. Geophys. Res.*, 83, 5361-5375, 1978.
- Morgan, J. P., and W. H. F. Smith, Flattening of the sea-floor depth-age curve as a response to asthenospheric flow, *Nature*, 359, 524-527, 1992.
- Minster, J. B., and T. H. Jordan, Present-day plate motions, *J. Geophys. Res.*, 83, 5331-5354, 1978.
- National Geophysical Data Center, ETOPO-5 bathymetry and topography data, *Data Announc. 88-MGG-02*, Natl. Oceanic and Atmos. Admin., Boulder, Colo., 1988.
- Oxburgh, E. R., and E. M. Parmentier, Compositional and density stratification in the oceanic lithosphere - causes and consequences, *J. Geol. Soc. Lon.*, 133, 313-355, 1977.
- Parsons, B., and F. M. Richter, A relation between driving force and geoid anomaly associated with the mid-ocean ridges, *Earth Planet. Sci. Lett.*, 51, 445-450, 1980.
- Parsons, B., and J. G. Sclater, An analysis of the variation of ocean floor bathymetry and heat flow with age, *J. Geophys. Res.*, 82, 803-827, 1977.
- Richardson, R. M., Ridge forces, absolute plate motions, and the intraplate stress field, *J. Geophys. Res.*, 97, 11739-11749, 1992.
- Richardson, R. M., and D. D. Coblenz, Potential energy arguments about the reference tectonic state (abstract), *EOS Trans. AGU, Fall Meeting Suppl.*, 73, 562, 1992.
- Richardson, R. M., and B. E. Cox, Evolution of oceanic lithosphere: A driving force study of the Nazca plate, *J. Geophys. Res.*, 89, 10,043-10,052, 1984.
- Richardson, R. M., and L. M. Reding, North American plate dynamics, *J. Geophys. Res.*, 96, 12,201-12,223, 1991.
- Richardson, R. M., S. C. Solomon, and N. H. Sleep, Tectonic stress in the plates, *Rev. Geophys.*, 17, 981-1019, 1979.
- Royer, J.-Y., R. D. Mueller, L. M. Gahagan, L. A. Lawyer, C. L. Mayes, D. Nuernberg and J. G. Sclater, A global isochron chart, *Tech. Rep.*, 117, 38 pp., Univ. of Tex. Inst. for Geophy., Austin, Texas, 1992.
- Sandiford, M., and R. Powell, Some isostatic and thermal consequences of the vertical strain geometry in convergent orogens, *Earth Planet. Sci. Lett.*, 98, 154-165, 1990.
- Sandiford, M., and R. Powell, Isostatic and thermal constraints on the evolution of high temperature low pressure metamorphic terrains in convergent orogens, *J. Metamorph. Geol.*, 9, 333-340, 1991.
- Sandwell, D. T., and W. H. F. Smith, Global marine gravity from ERS-1, GEOSAT and SEASAT reveals new tectonic fabric (abstract), *EOS Trans. AGU, Fall Meeting Suppl.*, 73, 133, 1992.
- Smith, W. H. F., On the accuracy of digital bathymetric data, *J. Geophys. Res.*, 98, 9591-9603, 1993.
- Sonder, L. J., P. C. England, B. P. Wernicke, and R. L. Christiansen, A physical model for Cenozoic extension of western North America, in *Continental Extensional Tectonics*, edited by M. P. Coward, J. F. Dewey, and P. L. Hancock, *Geol. Soc. Spec. Publ. London*, 28, 187-201, 1987.
- Turcotte, D. L., Mechanisms of crustal deformation, *J. Geol. Soc. London*, 140, 701-724, 1983.
- Turcotte, D. L., and G. Schubert, *Geodynamics: Applications of Continuum Physics to Geological Problems*, 450 pp., John Wiley, New York, 1982.
- Turcotte, D. L., W. F. Haxby, and J. R. Ockendon, Lithospheric instabilities, in *Island Arcs, Deep Sea Trenches, and Back-arc Basins*, Maurice Ewing Ser., vol. 1, edited by M. Talwani and W.C. Pitman III, pp. 62-69, AGU, Washington, D. C., 1977.
- Turcotte, D. L., and D. C. McAdoo, Geoid Anomalies and the thickness of the lithosphere, *J. Geophys. Res.*, 84, 2381-2387, 1979.
- White, R. S., D. McKenzie, and R. K. O'Neill, Oceanic crustal thickness from seismic measurements and rare Earth element inversions, *J. Geophys. Res.*, 97, 19,683-19,715, 1992.
- Wortel, M. J. R., M. J. N. Remkes, R. Govers, S. A. P. L. Cloetingh, and P. Th. Meijer, Dynamics of the lithosphere and the intraplate stress field, *Philos. Trans. R. Soc. London, Ser. A*, 337, 111-126, 1991.
- Zhou, S., and M. Sandiford, On the stability of isostatically compensated mountain belts, *J. Geophys. Res.*, 97, 14,207-14,221, 1992.
- Zoback, M. D. et al., Upper-crustal strength inferred from stress measurements to 6 km depth in the KTB borehole, *Nature*, 365, 633-635, 1993.
- Zoback, M. L. et al., First- and second-order patterns of stresses in the lithosphere: The World Stress Map project, *J. Geophys. Res.*, 97, 11,703-11,729, 1992.
- Zoback, M. L., and M. Magee, Stress magnitudes in the crust: Constraints from stress orientation and relative magnitude data, *Philos. Trans. R. Soc. London A*, 337, 181-194, 1991.

D. D. Coblenz and R. M. Richardson,
Southern Arizona Seismic Observatory,
Department of Geosciences, University of
Arizona, Tucson, AZ 85721.

M. Sandiford, Department of Geology and
Geophysics, University of Adelaide,
Adelaide, SA 5005, Australia.

(received September 7, 1993;
revised April 12, 1994;
accepted April 19, 1994.)